

## Two-pronged events in ${}^4\text{He}$ - $p$ collisions at $8.56 \text{ GeV}/c$ ${}^4\text{He}$ incident momentum

V. V. Glagolev, R. M. Lebedev, I. S. Saitov, V. N. Streltsov, and L. I. Zuravleva  
*Joint Institute for Nuclear Research, Dubna, Union of Soviet Socialist Republics*

A. N. Gorbunov and K. U. Khayretdinov  
*P. N. Lebedev Physical Institute of the Academy of Science, Moscow, Union of Soviet Socialist Republics*

G. Martinska, I. Patočka, and M. Seman  
*Institute for Experimental Physics, Košice, Czechoslovakia*

H. Braun, A. Fridman, J. P. Gerber, H. Johnstad, P. Juillot, and A. Michalon  
*Centre de Recherches Nucléaires, Strasbourg, France*

B. S. Aladashvili and M. S. Nioradze  
*Tbilisi University, Tbilisi, Union of Soviet Socialist Republics*

T. Siemiarczuk, T. Sobczak, J. Stepaniak, and P. Zielinski  
*Institute of Nuclear Research, Warsaw, Poland*  
 (Received 25 April 1977)

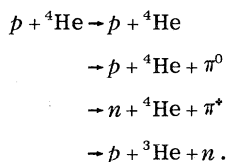
We have studied  ${}^4\text{He}$ - $p$  collisions at a  ${}^4\text{He}$  incident momentum of  $8.56 \text{ GeV}/c$  using the 1 m Dubna bubble chamber. The  $p$ - ${}^4\text{He}$  elastic scattering, the coherent  $p + {}^4\text{He} \rightarrow N + {}^4\text{He} + \pi$  production and the breakup reaction  $p + {}^4\text{He} \rightarrow p + {}^3\text{He} + n$  have been investigated. Cross sections and production features are presented. From the breakup reaction, subsamples of events in which a  ${}^3\text{He}$  or a  $n$  appear as spectators were selected. These events were used to study the virtual  $pn \rightarrow pn$  and  $p + {}^3\text{He} \rightarrow p + {}^3\text{He}$  scattering.

[NUCLEAR REACTIONS  ${}^4\text{He}(p, p)$ ,  $(p, p\pi^0)$ ,  $(p, n\pi^+)$ ,  $(p, pn)$ ,  $E = 1.41 \text{ GeV}$ ; bubble chamber; measured  $\sigma$ ; deduced  $n(p, p)$ ,  ${}^3\text{He}(p, p)$ .]

### I. INTRODUCTION AND EXPERIMENTAL PROCEDURE

In this work we present results on two-pronged events obtained in  ${}^4\text{He} + p$  collisions at an incident  ${}^4\text{He}$  momentum of  $8.56 \text{ GeV}/c$ , corresponding to a proton momentum of  $2.15 \text{ GeV}/c$  in the  ${}^4\text{He}$  rest system. The experiment was carried out at Dubna using the 1 m hydrogen bubble chamber. About 180 000 pictures were taken and scanned twice for all topologies, the scanning efficiency for two-pronged events was  $(98 \pm 2)\%$ . The present work is based on a fraction of the information contained in the film, namely, 1491 well measured and identified two-pronged events.

We have investigated the reactions



Using a  ${}^4\text{He}$  beam gives access to the kinematical region in which the four-momentum transfer between the incident  ${}^4\text{He}$  and the outgoing  ${}^4\text{He}$  or  ${}^3\text{He}$  is small. Moreover, the event selection is simplified as the outgoing  ${}^4\text{He}$  or  ${}^3\text{He}$  has a momen-

tum which is very different from the other emitted particle. This can be seen from Fig. 1 which presents the measured laboratory momentum for all outgoing tracks. The two bumps in this figure are due to  ${}^3\text{He}$  and  ${}^4\text{He}$  tracks, verified from the uniquely identified events. Thus a cut in momen-

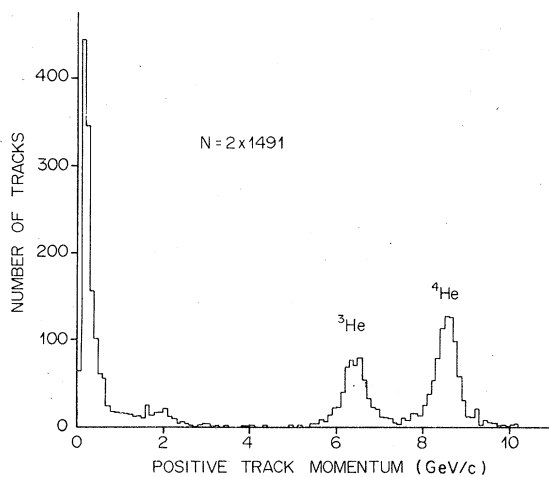


FIG. 1. Measured momentum distribution obtained from 1491 two-pronged events. The observed bumps correspond to  ${}^3\text{He}$  and  ${}^4\text{He}$  tracks.

tum on the fastest outgoing particle can solve most of the ambiguity problems, while further cuts on missing mass squared and  $\chi^2$  probability provide clean samples of events.

We have corrected our various samples for scanning efficiency and for loss of short tracks and steeply dipping tracks. These losses were estimated by studying the azimuthal distribution of the short positive track around the incident  ${}^4\text{He}$  direction. A correction of about 13% was obtained for inelastic two-pronged events. For the elastic scattering a correction of 24% was applied on the events having a proton momentum greater than 100 MeV/c. Below this value the losses were estimated by fitting the experimental distribution of the four-momentum transfer between the initial and outgoing  ${}^4\text{He}$  with an exponential function (see Sec. II). We thus obtain the cross sections of the studied channels as indicated in Table I where the errors are of statistical nature. The study of these channels will be made in the next sections. Section II will treat the elastic scattering and the  $p + {}^4\text{He} \rightarrow N + {}^4\text{He} + \pi$  coherent production. The breakup reaction  $p + {}^4\text{He} \rightarrow p + {}^3\text{He} + n$  is studied in Sec. III.

## II. ELASTIC SCATTERING AND COHERENT PRODUCTION

In Fig. 2 we present the differential elastic cross section as a function of  $|t|$ , where  $t$  is the four-momentum transfer between the initial and final  ${}^4\text{He}$ . The error bars shown in Fig. 2 represent statistical errors only and do not include the error in the cross-section scale for absolute normalization which is estimated to be less than 8%. The experimental points were fitted to an exponential function  $e^{bt}$  leading to a slope  $b = 27.4 \pm 1.5$   $(\text{GeV}/c)^{-2}$ . The value of the slope found in the

TABLE I. Cross sections obtained for the studied channels.

Reaction	Cross section (mb)
${}^4\text{He} + p \rightarrow {}^4\text{He} + p$	36 $\pm$ 3
${}^4\text{He} + p \rightarrow {}^4\text{He} + p + \pi^0$	1.06 $\pm$ 0.18
${}^4\text{He} + p \rightarrow {}^4\text{He} + n + \pi^+$	1.74 $\pm$ 0.23
${}^4\text{He} + p \rightarrow {}^4\text{He} + N + \pi$	2.80 $\pm$ 0.40
${}^4\text{He} + p \rightarrow {}^3\text{He} + p + n$	11.0 $\pm$ 0.5
${}^4\text{He} + p \rightarrow {}^3\text{He}_s + p + n$	9.7 $\pm$ 0.5
${}^4\text{He} + p \rightarrow n_s + {}^3\text{He} + p$	1.3 $\pm$ 0.2
$pn \rightarrow pn$	24.0 $\pm$ 1.2 <sup>a</sup>
	30.4 $\pm$ 1.5 <sup>a</sup>
Optical theorem estimate of total cross section	148 $\pm$ 7

<sup>a</sup> The first value was estimated without taking into account multiple scattering corrections while a crude correction was made to obtain the second value.

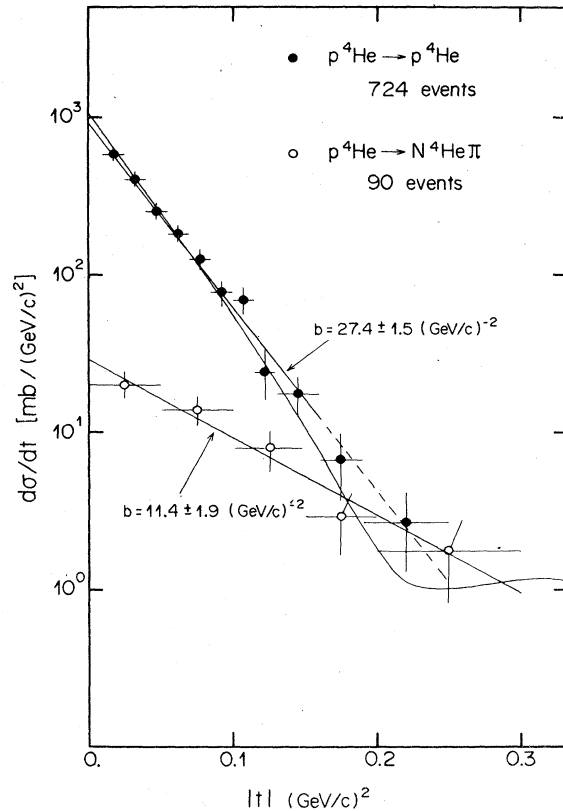


FIG. 2. The distribution of four-momentum transfer  $|t|$  between the initial and outgoing  ${}^4\text{He}$  for the  $p + {}^4\text{He} \rightarrow p + {}^4\text{He}$  and  $p + {}^4\text{He} \rightarrow N + {}^4\text{He} + \pi$  reactions. The data were fitted with  $e^{bt}$  functions and also by using the Glauber formalism for the elastic scattering.

present work is very close to those obtained in  $p + {}^4\text{He}$  elastic scattering at 1.70, 1.75, 1.87, and 3.49 GeV/c incident momentum<sup>1</sup> [ $b \approx 30$   $(\text{GeV}/c)^{-2}$  in the  $0.03 < |t| < 0.16$   $(\text{GeV}/c)^2$  range]. Unfortunately no quantitative study of the total elastic cross sections versus incident momentum can be made as the published data do not contain estimates of elastic cross sections. However, the comparison of the absolute values of the  $d\sigma/dt$  data in the  $|t| \sim 0.1$   $(\text{GeV}/c)^2$  region show that our elastic cross section is slightly below that observed at 1.75 and 1.87 GeV/c.<sup>1</sup> In contrast the elastic cross sections obtained from earlier measurements at 1.20, 1.26, 1.37, and 1.66 GeV/c (Ref. 2) are smaller than our value at 2.15 GeV/c. The fluctuations observed in the differential cross sections show that further measurement will certainly be useful. We also attempted to fit the elastic differential cross section using the Glauber multiple scattering theory<sup>3</sup> and obtained a rather good agreement with our data. In any case, data beyond the calculated minimum (see Fig. 2) should be accumulated in order to adjust the parameters en-

tering into the Glauber formula. Assuming that the  ${}^4\text{He}+p$  elastic scattering is purely imaginary, we obtain the optical theorem estimate for the total cross section, namely  $\sigma_{\text{tot}} = 148 \pm 7$  mb.

Because of the small statistics available in the coherent production, we added the events belonging to the  $p+{}^4\text{He} \rightarrow p+{}^4\text{He}+\pi^0$  and  $p+{}^4\text{He} \rightarrow n+{}^4\text{He}+\pi^+$  reactions to study the  $N+{}^4\text{He}+\pi$  final state. In fact the cross sections of the above two reactions are related by Clebsch-Gordan coefficients, i.e.,

$$\frac{\sigma(p+{}^4\text{He} \rightarrow n+{}^4\text{He}+\pi^+)}{\sigma(p+{}^4\text{He} \rightarrow p+{}^4\text{He}+\pi^0)} = 2.$$

As indicated in Table I our results are compatible within errors with this ratio.

Figure 2 presents the distribution of the four-momentum transfer  $|t|$  between the initial and outgoing  ${}^4\text{He}$  in the  $p+{}^4\text{He} \rightarrow N+{}^4\text{He}+\pi$  reaction. Fitting this distribution with an  $e^{bt}$  function, we obtain a slope  $b = 11.4 \pm 1.9$   $(\text{GeV}/c)^{-2}$ . As no  ${}^4\text{He}+p$  and no  $p\bar{d}$  data are available for comparison with our results, we have used  $p\bar{d}$  data at 5.55  $\text{GeV}/c$ .<sup>4</sup> Indeed it has been shown that coherent production on deuterium does not depend strongly on whether the reaction is induced by  $p$  or  $\bar{p}$ ,<sup>5</sup> and no sizable energy dependence is observed in the shape of the differential cross section. Using these  $p\bar{d}$  data we observe that the ratio of elastic cross section to that of one- $\pi$  production has nearly the same value  $\sim 13$  for  ${}^4\text{He}+p$  and for  $p\bar{d}$  interactions (see Table I).

The  $\pi+{}^4\text{He}$  and  $N+\pi$  effective mass distributions are displayed in Fig. 3 and compared with peripheral phase space predictions. This phase space is obtained by weighting each event generated with a Monte Carlo method by an  $e^{bt}$  factor. Here  $b$  is the experimental value previously determined. One notices a small accumulation of events above

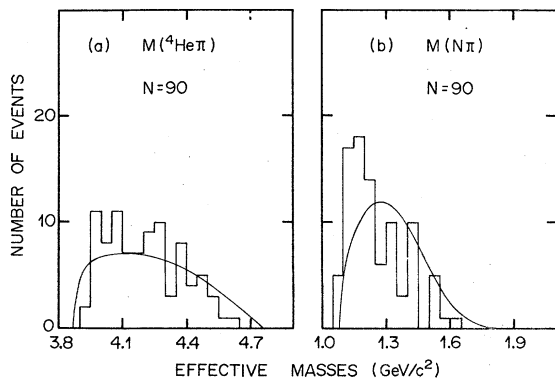


FIG. 3. Distributions of the  ${}^4\text{He}+\pi$  (a) and the  $N+\pi$  (b) effective masses. The full curves represent peripheral phase space normalized to  $N=90$ , the total number of events.

the phase space in the  $\pi+{}^4\text{He}$  effective mass distribution. The statistics are too small to detect an  ${}^4\text{He}^*$  which would have a mass of about 4  $\text{GeV}/c^2$  if it has the same origin as the  $d^*$  observed in coherent interactions on deuterium.<sup>6</sup> In the  $N\pi$  effective mass distribution, one observes a bump at low-mass values similar to those seen in other coherent production as for instance in the  $\bar{p}+d \rightarrow \bar{n}+d+\pi$  reaction at 5.55  $\text{GeV}/c$ .<sup>4</sup>

### III. BREAKUP REACTION $p+{}^4\text{He} \rightarrow p+{}^3\text{He}+n$

This reaction has the interesting property that it offers the possibility of learning something about the internal structure of the  ${}^4\text{He}$ . In particular one may ask if the spectator scheme can be applied to the breakup reaction. To study this question we plot in Fig. 4 the angular distribution and the momentum of the so-called  $n$  and  ${}^3\text{He}$  spectators (denoted by  $n_s$  and  ${}^3\text{He}_s$ ) in the  ${}^4\text{He}$  rest frame, where the angular distribution is defined with respect to the initial proton momentum. The  ${}^3\text{He}$  ( $n$ ) is defined as a spectator when its momentum in the  ${}^4\text{He}$  rest frame is smaller than that of the  $n$  ( ${}^3\text{He}$ ). As can be seen from Fig. 4 the  $n_s$  and  ${}^3\text{He}_s$  present the characteristic spectator distributions, namely, the  $n_s$  and  ${}^3\text{He}_s$  tend to be emitted isotropically and with small momentum. The momentum distributions are compared with the calculations of Kopeliovitch and Potashnikova<sup>7</sup> based on the Bassel-Wilkin wave function of the  ${}^4\text{He}$  particle.<sup>8</sup> Finally we show in Figs. 4(c) and 4(f) the distribution of the c.m. energy introduced by the Fermi motion inside the  ${}^4\text{He}$  for the virtual  $pn \rightarrow pn$  and  $p+{}^3\text{He} \rightarrow p+{}^3\text{He}$  scattering. The curves shown in Fig. 4 are obtained from the spectator momentum distribution given in Ref. 7.

The four-momentum transfer between the incident and outgoing  $p$  in the  $p+{}^4\text{He} \rightarrow {}^3\text{He}_s+pn$  and the  $p+{}^4\text{He} \rightarrow n_s+p+{}^3\text{He}$  is presented in Figs. 5 and 6. The fact that these distributions tend to zero when  $|t| \rightarrow 0$  is due to the  ${}^4\text{He}$  binding energy. Indeed in this region, virtual  $pn$  or  $p+{}^3\text{He}$  scattering cannot occur since a fraction of the four-momentum transfer is always needed to break up the  ${}^4\text{He}$ .<sup>9</sup> Thus apart from the  $|t| \approx 0$  region, the distributions shown in Figs. 5 and 6 are intended to describe the  $pn \rightarrow pn$  and  $p+{}^3\text{He} \rightarrow p+{}^3\text{He}$  virtual scattering. The statistics for this last reaction are small. Nevertheless, we see that the four-momentum transfer is peaked toward low values. For the  $pn \rightarrow pn$  case, we observe the diffraction peak as well as the charge exchange process  $pn \rightarrow np$ . The backward scattering can be seen better in the insert of Fig. 5 which presents the distribution of  $|u|$ , where  $u$  is the four-momentum transfer between the initial  $p$  and the final  $n$ . By fitting the small  $|t|$  and  $|u|$  re-

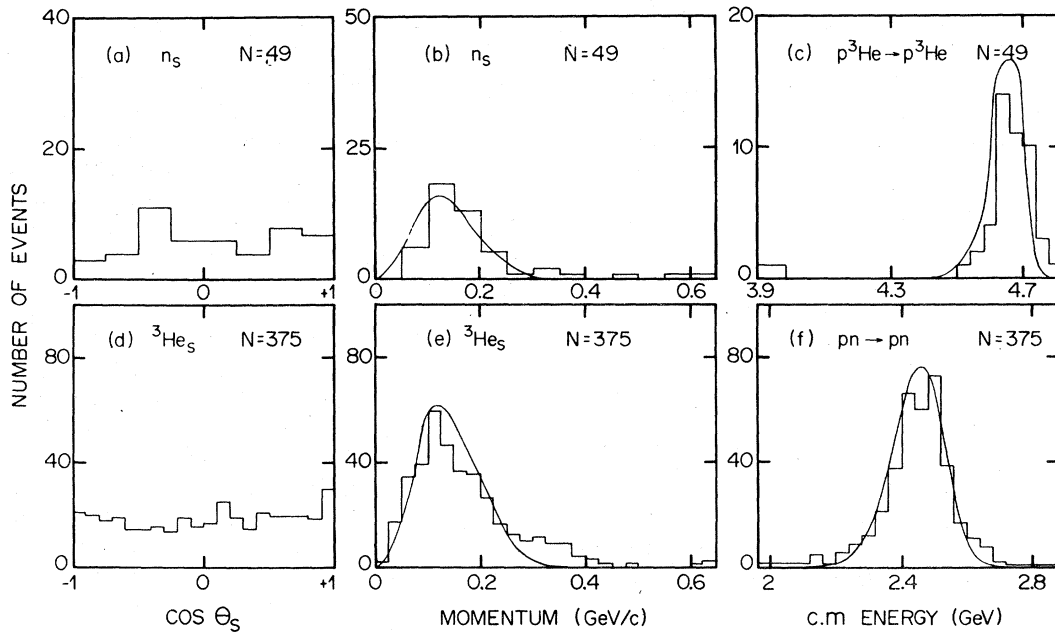


FIG. 4. The angular [(a) and (d)] and momentum [(b) and (e)] distributions of the  $n_s$  and  ${}^3\text{He}_s$  spectators. In (c) and (f) are represented the c.m. energy distributions due to the Fermi motion for the  $p+{}^3\text{He} \rightarrow p+{}^3\text{He}$  and  $pn \rightarrow pn$  virtual scattering.

gions with exponential functions we find practically the same slopes, i.e.,  $4.5 \pm 0.5 (\text{GeV}/c)^{-2}$  and  $4.1 \pm 1.0 (\text{GeV}/c)^{-2}$ , respectively.<sup>10</sup> One notices that the slopes obtained for the diffraction peak are similar to that deduced from  $pd$  interactions at  $\sim 2 \text{ GeV}/c$

(Ref. 11). Nevertheless, we want to emphasize that it may be much more convenient to use  $p^4\text{He}$  collisions instead of  $pd$  ones for studying  $pn$  scattering. Indeed because of the diffractive nature of the elastic scattering, the recoiling  $n$  in

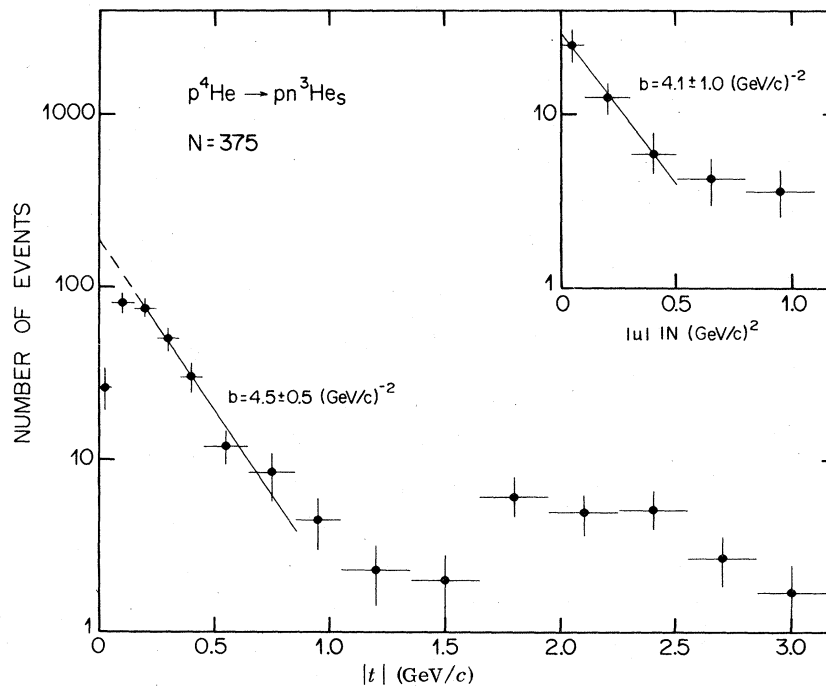


FIG. 5. The  $|t|$  and  $|u|$  distributions for the virtual  $pn \rightarrow pn$  scattering. Here  $t$  and  $u$  are the four-momentum transfer between the initial  $p$  and the final  $p$  or  $n$ , respectively. The full lines were obtained by fitting the data with  $e^{bt}$  functions.

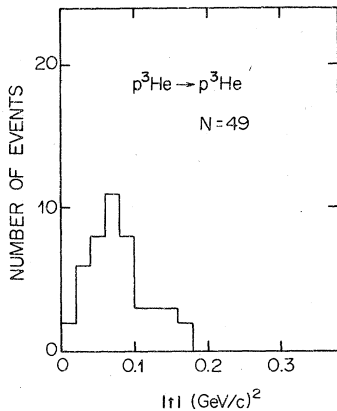


FIG. 6. The  $|t|$  distribution for virtual  $p + {}^3\text{He} \rightarrow p + {}^3\text{He}$  scattering in the reaction  $p + {}^4\text{He} \rightarrow n_s p + {}^3\text{He}$ .

$pn \rightarrow pn$  often has a momentum similar to that of the spectator proton. This may lead to difficulties whenever the spectator model is applied to the  $pd \rightarrow ppn$  reaction.<sup>12</sup> Moreover, the fact that the two slow nucleons in this reaction have comparable momenta leads to the suppression of some kinematical configurations as a consequence of the generalized exclusion principle.<sup>13</sup> Such a situation does not occur with the  ${}^3\text{He}_s$  events. In addition we would also like to point out that the virtual neutron target mass is not too far from the real neutron mass. Indeed, if we assume that the  ${}^3\text{He}$  is on its mass shell when the interaction occurs, we obtain that the virtual neutron mass follows a distribution with an average of  $0.889 \text{ GeV}/c^2$  and a dispersion of  $0.045 \text{ GeV}/c^2$ .

Although the spectator scheme may be applied to the breakup reaction  $p + {}^4\text{He} \rightarrow {}^3\text{He} + pn$ , some correlation exists between the outgoing particles and the spectator. This can be seen by examining for instance the Treiman-Yang  $\varphi$  angle, defined in Fig. 7. The asymmetry parameter, plotted in Fig. 8, is the ratio of the number of cases where  $\varphi > \pi/2$  to the number where  $\varphi \leq \pi/2$  as a function of the spectator momentum. A significant deviation from zero is seen when the momentum of the spectator increases. This correlation cannot be explained by a kinematical effect.<sup>14</sup> The same result has also been observed in  $dp$  interactions at  $3.3 \text{ GeV}/c$  (Ref. 15). By comparing the  $dp$  interaction with our results, it appears that the asymmetry parameters tend to have the same dependence on the spectator momentum.

In order to calculate the  $np \rightarrow np$  cross section from the observed  $p + {}^4\text{He} \rightarrow {}^3\text{He}_s + pn$  reaction we have to use a model. We will assume that a bound proton in the  ${}^4\text{He}$  has the same probability ( $P$ ) as the bound neutron of hitting the proton target, neglecting off mass shell and screening effects.

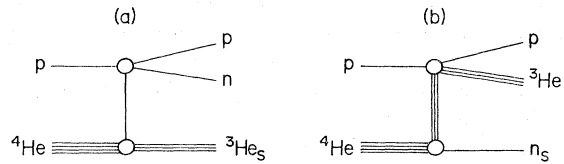


FIG. 7. Schematic representation of the  $p + {}^4\text{He} \rightarrow {}^3\text{He}_s + pn$  [(a)] and  $p + {}^4\text{He} \rightarrow n_s + {}^3\text{He} + p$  [(b)] reactions. The Treiman-Yang angle is defined in (a) [(b)] as the angle between the normals of the planes formed by the momenta of the outgoing  $p$  and  $n$  ( ${}^3\text{He}$ ) and by the momenta of the  ${}^4\text{He}$  and  ${}^3\text{He}_s$  ( $n_s$ ), all momenta expressed in the initial  $p$  rest frame.

Using these assumptions and by extrapolating the elastic  $np$  differential cross section toward low  $|t|$  with the help of the fitted  $e^{bt}$  function, we obtain an elastic  $np$  cross section of  $\sigma = 24.0 \pm 1.2 \text{ mb}$ . In a rather simplified manner one can also take into account multiple scattering processes (elastic or inelastic) inside the  ${}^4\text{He}$ . In other words no multiple scattering has to occur if we want to observe the  $np \rightarrow np$  reaction. If  $P'$  is the probability that a second scattering will be made inside the  ${}^4\text{He}$ , the overall probability of observing an elastic event in the  $p + {}^4\text{He} \rightarrow {}^3\text{He}_s + pn$  reaction is  $2P(1 - P')^3$ . Using an  $NN$  total cross section of  $44.6 \text{ mb}$  and still correcting the  $|t|$  distribution for small  $|t|$ , we obtain an elastic  $np$  cross section of  $30.4 \pm 1.5 \text{ mb}$ .

The method we used for calculating the cross section is based on many assumptions, in particular on the fact that  $P$  and  $P'$  do not depend on the momentum configuration of the interacting nucleons. Moreover, the method used to correct for multiple scattering effects is certainly too crude for accurate estimates of the cross section.

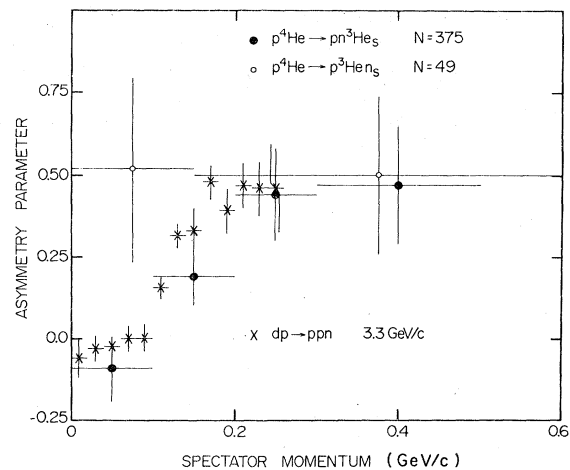


FIG. 8. The asymmetry parameter in the Treiman-Yang angle (see text) as a function of the spectator momentum.

Therefore the obtained cross sections have to be considered as estimates only. However, the  ${}^3\text{He}_s$  events allow one to study the general features of  $np$  interactions.

No cross-section estimates were made for the  $p+{}^3\text{He}\rightarrow p+{}^3\text{He}$  elastic scattering. Indeed it is hard to believe that the same probability governs the interaction of a proton with groups of three nucleons whatever their charge and their momentum configuration.

#### IV. CONCLUSIONS

From the study of the two-pronged events we obtain results on the reactions  $p+{}^4\text{He}\rightarrow p+{}^4\text{He}$ ,  $p+{}^4\text{He}\rightarrow N+{}^4\text{He}+\pi$ , and  $p+{}^4\text{He}\rightarrow p+{}^3\text{He}+n$ . We have evaluated the cross sections for these channels and investigated their production features.

The  $p+{}^4\text{He}$  elastic scattering can be characterized by a steep four-momentum transfer distribution. The  $p+{}^4\text{He}\rightarrow N+{}^4\text{He}+\pi$  channel presents

some accumulation of events in the low  $\pi+{}^4\text{He}$  ( $\sim 4\text{ GeV}/c^2$ ) and  $N\pi$  ( $\sim 1.2\text{ GeV}/c^2$ ) mass regions. The statistics are yet too small to give a quantitative description of these effects.

Using the breakup reaction we isolated sub-samples of events with spectators, i.e.,  ${}^3\text{He}_s$  or  $n_s$ . We also note that correlation is observed between the spectator and the outgoing particles, a fact already observed in  $dp$  interactions. The value of the asymmetry parameter in the Treiman-Yang  $\varphi$  angle increases with the momentum of the spectator, this does not appear to be a kinematical effect.

By means of the breakup events we also studied the virtual  $pn\rightarrow pn$  and  $p+{}^3\text{He}\rightarrow p+{}^3\text{He}$  elastic scattering. Although the cross-section determination for these processes is subject to some difficulty, we investigated the  $pn$  and  $p+{}^3\text{He}$  elastic differential cross section. In particular we obtained results on forward and backward  $pn$  elastic scattering.

<sup>1</sup>E. Aslanides *et al.*, Phys. Lett. **68B**, 221 (1977); G. Igo *et al.*, International Conference on High Energy Physics and Nuclear Structure, Zürich, 1977 (unpublished).

<sup>2</sup>E. T. Boschitz *et al.*, Phys. Rev. Lett. **20**, 1116 (1968); M. S. Kozodaev *et al.*, Zh. Eksp. Teor. Fiz. **38**, 409 (1960) [Sov. Phys.-JETP **11**, 511 (1960)]; P. McManigal, Phys. Rev. **137**, 620 (1965); B. L. Riddiford and A. W. Williams, Proc. R. Soc. **A257**, 316 (1960).

<sup>3</sup>We took the Glauber formula given by W. Czyz and L. Lesniak, Phys. Lett. **24**, 227 (1967), with a real to imaginary part of the  $NN$  elastic scattering amplitude of  $-0.5$  and a slope  $b=5\text{ (GeV}/c)^{-2}$  for the  $NN$  elastic differential cross section.

<sup>4</sup>See for instance, H. Braun *et al.*, Phys. Rev. D **8**, 2765 (1973), and reference quoted therein.

<sup>5</sup>H. Braun *et al.*, Nuovo Cimento **35**, 405 (1976); P. Juillot, in *Proceedings of the Third European Symposium on Antinucleon-Nucleon Interactions, Stockholm, 1976*, edited by G. Ekspong and Nilsson (Pergamon, New York, 1977), p. 403.

<sup>6</sup>See for instance, H. Braun *et al.*, Phys. Rev. D **2**, 1212

(1970).

<sup>7</sup>B. Z. Kopeliovitch and I. K. Potashnikova, Yad. Fiz. **13**, 1032 (1971) [Sov. J. Nucl. Phys. **13**, 592 (1971)].

<sup>8</sup>R. H. Bassel and C. Wilkin, Phys. Rev. **174**, 1179 (1968).

<sup>9</sup>V. Franco and R. J. Glauber, Phys. Rev. **142**, 1195 (1966).

<sup>10</sup>For very small  $|\mu|$  one generally finds steeper slopes than for the  $|t|$  distribution. Here, however, the statistics are too small to observe this effect.

<sup>11</sup>E. Coleman *et al.*, Phys. Rev. **164**, 1655 (1967).

<sup>12</sup>H. Braun *et al.*, Phys. Rev. D **10**, 3572 (1974).

<sup>13</sup>See for instance, A. Fridman, Fortschr. Phys. **22**, 243 (1975).

<sup>14</sup>This can be seen by generating  $p+{}^4\text{He}\rightarrow {}^3\text{He}_s+p+n$  events according to the experimental distribution of the four-momentum transfer between the initial and final  $p$  and by taking into account the Fermi motion of the  $n$  inside the  ${}^4\text{He}$ .

<sup>15</sup>B. S. Aladashvili *et al.*, J. Phys. G **3**, 7 (1977).